ELSEVIER

Chemical Engineering Journal 130 (2007) 147–152

Chemical Engineering Journal

www.elsevier.com/locate/cej

Measuring gas–liquid distribution in a pilot scale monolith reactor via an Industrial Tomography Scanner (ITS)

M.H. Al-Dahhan [a,*], A. Kemoun [a,e], A.R. Cartolano [b], S. Roy [a], R. Dobson [c], J. Williams [d]

[a] *Chemical Reaction Engineering Laboratory (CREL), Chemical Engineering Department, Washington University, St. Louis, MO 63130, USA*
[b] *Air Products and Chemicals Inc., Allentown, PA, USA*
[c] *Tracerco, Houston, TX, USA*
[d] *Corning Inc., NY, USA*
[e] *Chevron Texaco, Richmond, CA, USA*

Abstract

An Industrial Tomography Scanner (ITS) was designed and developed to study and quantify the phase distribution in a two-phase flow pilot scale monolith reactor that was 24 in. (0.60 m) in diameter and 192 in. (4.9 m) in height. The monolith reactor was operated co-current up-flow in the Taylor flow regime with water as the liquid phase and air as the gas phase. The cross-sectional holdup distributions were measured at three axial elevations. The operating conditions were selected to bracket commercial operating conditions for fixed bed monolithic reactor systems. The results show that ITS can capture the flow features in a large diameter column. Also the findings suggest the need for careful design of the internals of the reactor. Spatial resolution down to 1.5 cm was obtained so that gross phase maldistribution could be reliably observed. However, improvement is needed for the ITS to be effectively utilized in industry.

Keywords: Monolith; Industrial tomography; Flow distribution

1. Introduction

Solid catalyzed gas–liquid reactions have long been an important part of the chemical process industries. Monolith reactors (as multiphase reactors) are claimed to have several advantages: low pressure drop, excellent mass transfer properties, high surface/volume ratio, short diffusion distance, low axial dispersion, and ease of reactor scale-up, among others [1–4]. However, there are still a few drawbacks associated with monolith reactors. These include the high cost of manufacturing the structure and poor heat transfer.

Although, several researchers have studied monolith as a multiphase reactor, unfortunately, the technology is not yet at a level which can be widely implemented on industrial scales. One of the major hurdles in designing, scaling up, and operating a monolith reactor is the flow distribution characteristics, which are strongly dependent on the reactor scale and the inlet distribution of the gas and liquid phases. Recent studies have shown that monolith reactors of larger diameter operated in the Taylor flow regime could suffer from phase maldistribution at the reactor inlet, which then remains throughout the length of the reactor [5–7]. This maldistribution could reduce the productivity of monolith reactor, therefore, offsetting the advantages derived from superior mass transfer characteristics. It is noteworthy that in industrial pilot plant scale monolith reactors (diameter > 0.3 m) the characteristics of phase distribution are still unknown.

Therefore, in this study, gas–liquid distribution was measured and characterized in a 2 ft (0.6 m) diameter pilot plant scale reactor packed with monolith elements. The pilot unit was installed at an Air Products and Chemicals (APCI) facility, Pace, FL. An Industrial Tomography Scanner (ITS) was designed and developed to visualize the phase distribution in the reactor cross-section at selected heights along its length. A version of such an ITS also was later developed by Tracerco to perform process diagnostics in large reactor configurations [8]. Such a fit-for-use tomography technique was found to provide important density distribution information inside a flow reactor at much less cost than other techniques.

* Corresponding author. Tel.: +1 314 935 7187; fax: +1 314 935 4832.
E-mail address: muthanna@che.wustl.edu (M.H. Al-Dahhan).

1385-8947/$ – see front matter © 2006 Elsevier B.V. All rights reserved.
doi:10.1016/j.cej.2006.06.022

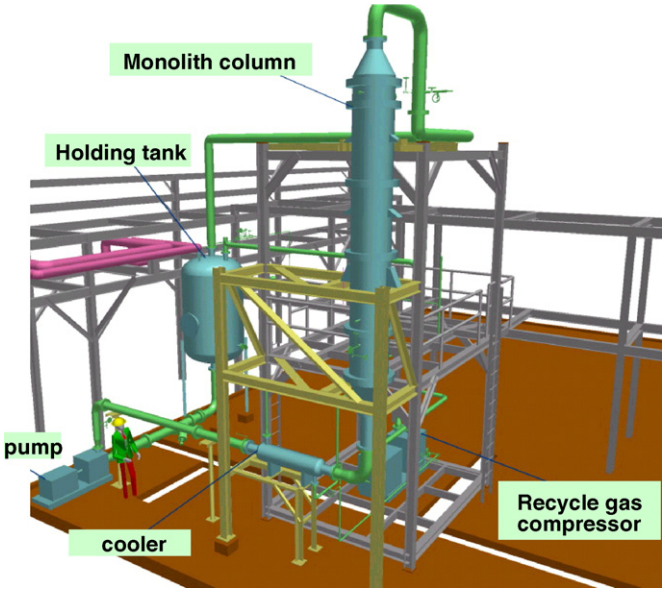

Fig. 1. Illustration of the pilot plant monolith unit.

2. Experimental setup

2.1. Monolith flow system

The pilot size monolith column used in this work has an inner diameter of 23(3/4) in. (0.60 m), a (1/4) in. (0.006 m) steel wall thickness, and a height of 192 in. (4.9 m). An illustration of the pilot plant is shown in Fig. 1. In the column housing the monolith bed, a distributor is mounted at the entrance to ensure a homogeneous two-phase flow distribution over the monolith packing. The monolith bed, which is 120 in. (3.05 m) long, was constructed of nominal 6 in. × 6 in. × 6 in. (0.15 m × 0.15 m × 0.15 m) cubes, glued into 2 ft (0.6 m) long strips (blocks), and shaped to fit inside the column. These strips were then stacked manually in an alternating 90°, 45° and 90° staggered pattern with respect to the strips orientation to prevent bypassing of the flow, as shown in Fig. 2. The monolith employed had a cell density of 400 cpsi (cells per square inch) and an open cross-flow area of 0.62. Fig. 3, a top view of the monolith column internals, illustrates the gaskets around the support and hold-down grids that prevent flow through the clearance between the monolith bed and the column wall. The monolith reactor was operated co-currently up-flow of gas and liquid phases in the Taylor flow regime with water as the liquid phase and air as the gas phase.

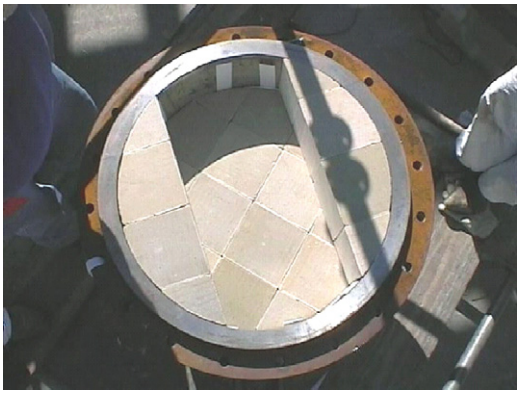

Fig. 2. Staggered pattern of the monolith strips (blocks) layers in the column.

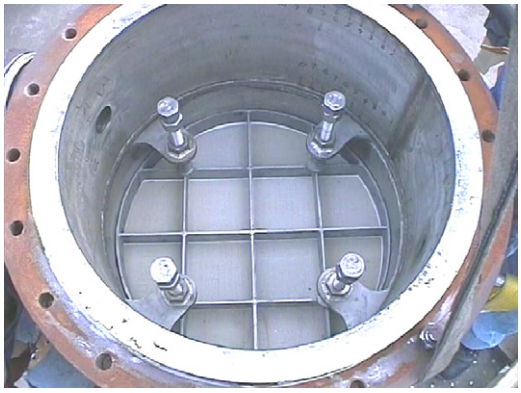

Fig. 3. Top view of the inner pilot plant scale monolith column.

2.2. Industrial Tomography Scanner design

The Industrial Tomography Scanner, designed by the Chemical Reaction Engineering Laboratory (CREL) at Washington University in St. Louis and constructed by Tracerco, is schematically shown in Fig. 4a and b. The ITS is an extension of the laboratory scale gamma ray computed tomography (CT) developed at CREL, details of which are given elsewhere [9,10].

The ITS was fixed on a platform consisting of two half-disc plates that can be mounted around a fixed column at various elevations. The disc plate was designed in such a way that the plate was always mounted concentric to the column center, and all the offsets between half-plate positioning were minimized. The outside overall diameter of this plate was 52 in. (1.3 m). On one of the half-plates a shielding lead block was mounted that contained a cesium (Cs) gamma ray radioactive source. The strength of the source was 400 mCi. The lead block of 6 in. × 8 in. × 3 in. (0.15 m × 0.2 m × 0.08 m) had a (1/2) in. (0.013 m) wide collimator and 80° view angle from the center of the source. The source was mounted at the center of the lead block as shown in Fig. 4a. The distance from the source center to the column wall was 6 in. (0.15 m). The inner diameter of the ITS was 25(1/2) in. (0.648 m) and the plate was 13(1/4) in. (0.34 m) wide.

On the other half-plate, opposite the source, detectors arranged on an arc were mounted. The location of the arc was around 33(3/4) in. (0.86 m) from the center of the radioactive source. The detectors were mounted in a block of lead of 5 in. × 3 in. × 3 in. (0.13 m × 0.08 m × 0.08 m) with a collimator (1/2) in. (0.013 m) in diameter and 2(1/2) in. (0.06 m) deep (Fig. 4a and b).

The resolution of the ITS is determined by the collimator window, detector/source distance, and the imperfect stability of the angular movement of the detector/source plate. The designed ITS gave an approximate resolution of 1.5 cm. Detectors were inserted in the lead block through holes 1(1/2) in. (0.038 m) in diameter × 3(1/2) in. (0.089 m) deep. The distance between

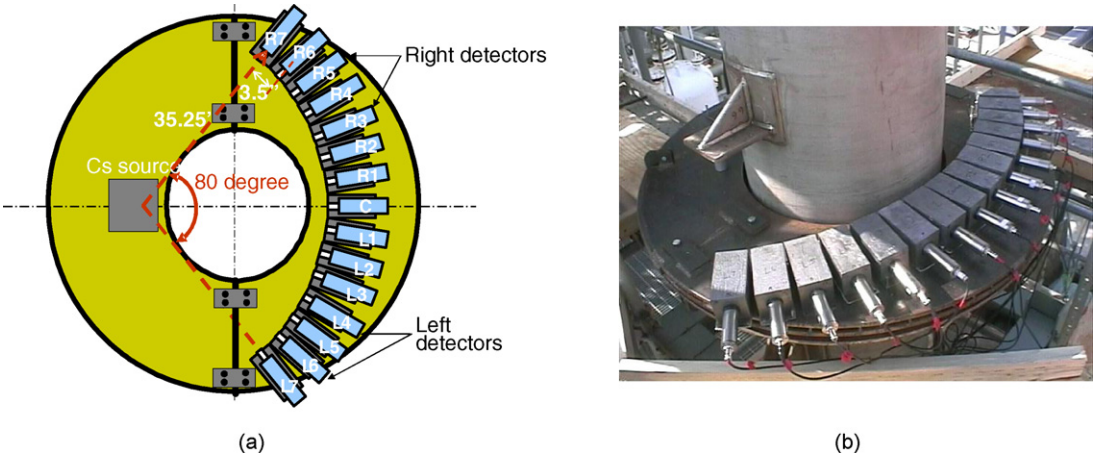

Fig. 4. (a) Schematic views of the Industrial Tomography Scanner (ITS) and (b) ITS mounted around the pilot monolith unit.

the detector center-face to its neighbor detector center-face was 3.5 in. (0.089 m). The total chord length from the radioactive source center to the detector center-face was 35.25 in. (0.9 m).

The entire source-detector assembly was rotated manually around the column, thereby, acquiring numerous projection data. The projection data were subsequently converted into cross-sectional attenuation profiles using a CREL developed Estimation-Maximization (EM) Algorithm [9]. The original EM algorithm was modified to incorporate the parameters of ITS. The attenuation profiles of the flow scans were subsequently converted into cross-sectional density profiles with the help of several reference scans. For details of the reconstruction steps, please refer to Ref. [11,12]. The pixel size used for the image reconstruction was 1.5 cm, which is the same as the ITS resolution. This resulted in a matrix of 40×40 (i,j) pixels to cover the entire monolith cross-section.

Due to the large dimensions of the ITS and the monolith column being scanned, and the difficulty associated with performing reference scans, the following assumptions were made:

- the stainless steel column is symmetric within manufacturing tolerances;
- the wall thickness of the steel column is uniform within manufacturing tolerances;
- the monolith is uniformly distributed in each cross section, and the cumulative thickness of partition walls that separate monolith channels is independent of the view angle.

In this work, the reference scans were mostly performed outside the pilot plant monolith bed using mock setups. Moreover, for several reference scans, only one view was obtained and the data was extrapolated to all 72 views needed for image reconstruction. In addition, the needed scans for dry monolith bed were computed from the scans of the monolith bed filled with liquid according to the validation performed by Al-Dahhan et al. [11]. Such steps and procedures are particularly useful for an industrial setting where equipment is unlikely to be available for the needed reference measurements that require a longer time.

2.3. Experimental conditions

The tomography scans were performed at three elevations (Table 1): the first at position 1, situated 15 in. (0.38 m) above the face of the bottom flange (just above the monolith entrance); the second at position 2, situated 59 in. (1.5 m) above the same flange (almost at the middle of the monolith); and the third at position 3, situated at 94.5 in. (2.4 m) above the same flange (before the exit of the monolith).

Nine operating flow conditions were examined. The conditions used to obtain the results at the three elevations are summarized in Table 1. Gas velocity was corrected for the inlet pressure. All gas and liquid velocities were within the Taylor flow regime [1].

3. Results and discussion

The reconstructed CT image yields 2-D map of the time averaged cross-sectional phase distribution at the scanned elevations for the studied operating conditions. Examples are shown in Fig. 5a for the relatively low superficial gas velocity of 31 cm/s (gas flow rate is about 42% of the total gas and liquid flow rate) and in Fig. 5b at the relatively high superficial gas velocity of 50 cm/s (gas flow rate is about 55% of the total gas and liquid flow rate).

The azimuthally averaged gas holdup profiles obtained at all flow conditions consistently showed a drop of gas holdup at $R > 0.25$ m (close to the wall), as shown in Fig. 6. This drop is due to the gaskets around the support and hold-down grids to prevent the flow from bypassing the monolith bed through the clearance between the bed and the column wall (Fig. 3). This clearly shows the need for careful design of the internals of the monolith bed.

It is evident from Fig. 6 that with increasing gas velocity, the ITS captures the increasing trend of the gas holdup. This trend was observed at all flow conditions and at all elevations. Larger gas holdup was observed at the top of the column than at the bottom, which could be due to both the expansion of the gas phase with column height and the increase in the superficial gas velocity from 37.5 to 48.7 cm/s, as shown in Fig. 7. It should

Table 1
Operating conditions for the ITS scans performed at 3 different elevations (positions)

Position 3 (94.5 inches (2.4 m) above the bottom flange)

Conditions	U_L (cm/s)	U_G (cm/s)
Condition 1	27.7	48.7
Condition 2	31.7	38.6
Condition 3	36.4	31.1

Position 2 (59 inches (1.5 m) above the bottom flange)

Conditions	U_L (cm/s)	U_G (cm/s)
Condition 1	27.7	44.4
Condition 2	31.7	34.5
Condition 3	35.6	30.2

Position 1 (15 inches (0.38 m) above the bottom flange)

Conditions	U_L (cm/s)	U_G (cm/s)
Condition 1	28.1	37.5
Condition 2	31.7	30.4
Condition 3	35.6	26.7

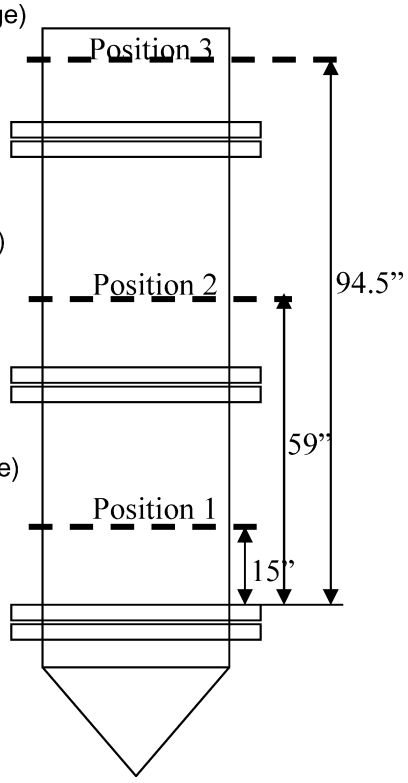

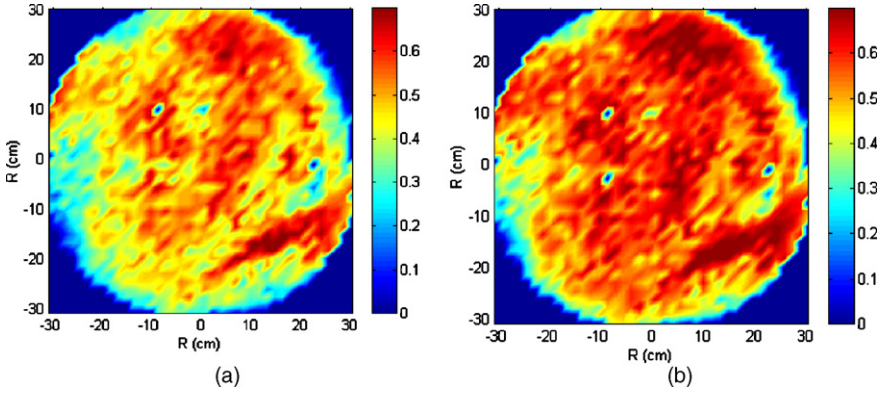

Fig. 5. Gas holdup distribution at: (a) low gas velocity (31 cm/s) and high liquid velocity (36.4 cm/s) and (b) high gas velocity (48.7 cm/s) and low liquid velocity (27.7 cm/s). Elevation: position 3 (Table 1).

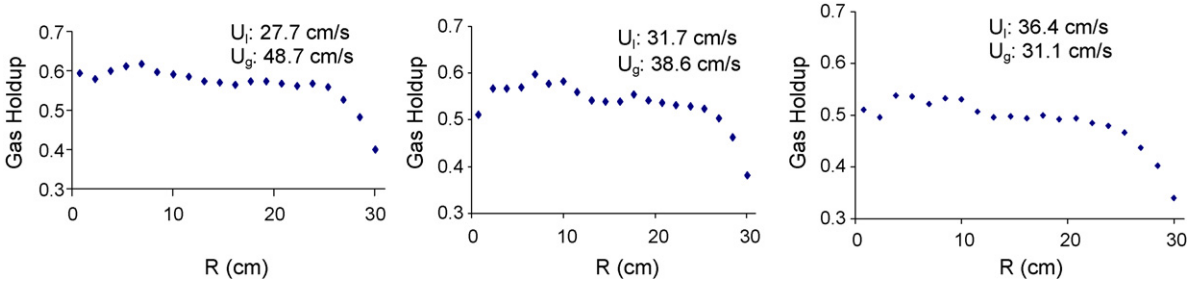

Fig. 6. Azimuthally averaged gas holdup radial profile at the highest position and decreasing gas velocity and increasing liquid velocity (from left to right) (position 3, Table 1).

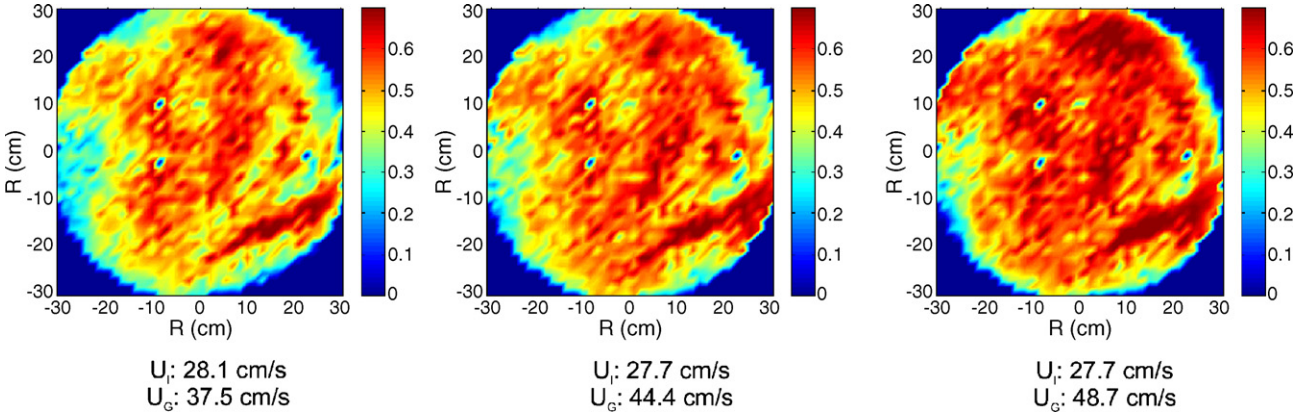

Fig. 7. Gas holdup distribution from position 1 to 3 at condition 1 (from bottom of the column to the top of the column).

be mentioned here that, due to experimental limitations (such as maintaining constant gas and liquid flow in the large diameter column), flow conditions changed from position to position, as shown in Table 1. The increase in gas holdup with column height could be expected in a non-reacting system. As the gas flows up, the static pressure decreases, allowing the gas to expand. However, due to the variation in the superficial gas velocity, it is not possible here to quantify the change in gas holdup due to gas phase expansion with column height.

3.1. Degree of phase uniformity

The degree of uniformity of the phase distribution at the conditions studied was assessed qualitatively by the standard deviation of gas holdup for the entire field, using an area-weighted standard deviation method [13].

$$\sigma = \sqrt{\sum_{i,j} \frac{A_{i,j}}{A_{\text{tot}}} \left(\frac{\varepsilon_{i,j} - \varepsilon_{\text{avg}}}{\varepsilon_{\text{avg}}} \right)^2}$$

$A_{i,j}$ and $\varepsilon_{i,j}$ are the area and holdup at each point in the two-dimensional field (column cross-section), respectively, A_{tot} the total area, and ε_{avg} is the azimuthally averaged holdup. Hence, a lower value of standard deviation indicates a better uniformity of phase distribution. The indices i and j represent the size of the image reconstruction matrix of 40×40 pixels and hence, they varied from 1 to 40.

The standard deviation (σ) values are tabulated in Table 2, and show that relatively better distribution was achieved at condition 2 and position 2 (Table 1).

Table 2
A summary of the standard deviation values (σ) for the phase distribution corresponding to the conditions of Table 1

	Position 1	Position 2	Position 3
Condition 1	23	16	17
Condition 2	23	15	19
Condition 3	25	18	25

4. Summary

It was shown that the Industrial Tomography Scanner is a viable tool to quantify the gas/liquid holdup distribution in packed beds and to detect any phase maldistribution. The ITS was able to detect the increasing gas holdup with increasing gas velocity and along the bed height. The resolution characteristics of the ITS were able to detect gross maldistribution of the system due to the presence of gaskets and hold-down grids. Accordingly, there is a need for careful design of the internals in order to avoid undesirable maldistribution. The degree of uniformity of the phase distribution decreases slightly with decrease in gas flow rate.

Acknowledgements

The financial support provided by Air Products and Chemicals, Inc., which made this work possible, is gratefully acknowledged. The authors also would like to thank Professor M.P. Dudukovic for his valuable comments and suggestions.

References

[1] S. Roy, T. Bauer, M.H. Al-Dahhan, P. Lehner, T. Turek, Monolith as multiphase reactor: a review, AIChE J. 50 (11) (2004).
[2] T. Boger, A.K. Heibel, C.M. Sorensen, Monolithic catalyst for the chemical industry, Ind. Eng. Chem. Res. 43 (16) (2004).
[3] T.A. Nijhuis, M.T. Kreutzer, A.C.J. Romijn, F. Kapteijn, J.A. Moulijn, Monolithic catalysts as more efficient three-phase reactors, Catal. Today 66 (2–4) (2001) 157–165.
[4] R.K. Edvinsson, M.J.J. Houterman, T. Vergunst, E. Grolman, J.A. Moulijn, Novel monolithic stirred reactor, AIChE J. 44 (11) (1998) 2459–2464.
[5] S. Roy, M.H. Al-Dahhan, Flow distribution characteristics of a gas–liquid monolith reactor, Catal. Today 105 (3–4) (2005) 396–400.
[6] N. Reinecke, D. Mewes, Flow regimes of two phase flow in monolith catalyst, in: 5th world congress on chemical engineering, San Diego, CA, 1996.
[7] L.F. Gladden, M.H.M. Lim, M.D. Mantle, A.J. Sederman, H. Stitt, MRI visualisation of two-phase flow in structured supports and trickle-bed reactors, Catal. Today 79–80 (2003) 203–210.
[8] M.W. Darwood, M. Davies, D. Godden, P. Jackson, K. James, E.H. Stitt, Development and implementation of gamma-ray tomography for field

applications, in: 3rd World Congress on Industrial Process Tomography, Banff, Canada, September, 2003, p. 207.
[9] S.B. Kumar, M.P. Dudukovic, J. Chaouki, F. Larachi, Computer Assisted Gamma and X-ray Tomography: Applications to Multiphase Flow Systems, Non-Invasive Monit Multiphase Flows, Elsevier, 1997, 47–103.
[10] S. Roy, A. Kemoun, M.H. Al-Dahhan, M.P. Dudukovic, T.B. Skourlis, F.M. Dautzenberg, Countercurrent flow distribution in structured packing via computed tomography, Chem. Eng. Process. 44 (2004) 59–69.
[11] M.H. Al-Dahhan, A. Kemoun, A.R. Cartolano, Phase distribution in an upflow monolith reactor using computed tomography, AIChE J. 52 (2) (2005) 745–753.
[12] J. Chen, R. Novica, M.H. Al-Dahhan, M.P. Dudukovic, Study of particle motion in packed/ebullated beds by computed tomography (CT) and computer automated radioactive particle tracking (CARPT), AIChE J. 47 (5) (2001) 994–1004.
[13] Y. Jiang, Flow Distribution and its impact on performance of packed-bed reactors, Ph.D. Thesis, Washington University, Missouri, 2000.